# Eastern Boundary Conditions and Weak Solutions of the Ideal Thermocline Equations

W. R. YOUNG

*Department of Earth, Atmospheric, and Planetary Sciences, Massachusetts Institute of Technology, Cambridge, MA 02139*

G. R. IERLEY

*Department of Mathematical and Computer Sciences, Michigan Technological University, Houghton, MI 49931*

(Manuscript received 16 January 1986, in final form 15 May 1986)

ABSTRACT

It is argued that the ideal fluid thermocline equations have "weak" (i.e., nondifferentiable) solutions that satisfy no mass-flux boundary conditions at the East. This conclusion is based on a local analysis of the eastern "corner" of a subtropical gyre. Specifically we suppose that the surface density is uniform while the density on the eastern boundary is either uniform (but different from that of the surface) or else is linearly stratified. The surface density is injected into the interior by specified Ekman pumping. In the absence of dissipation the resulting solution would have a discontinuity in density at some interior position. In the presence of small vertical density diffusion, this discontinuity is "smoothed" and becomes an internal boundary layer which separates the light fluid originating at the surface from the denser fluid which abuts the eastern boundary.

This solution, which is of the similarity type, illustrates the applicability of solutions of the ideal fluid thermocline problem with discontinuities. It is these discontinuities which enable ideal fluid solutions to satisfy eastern boundary conditions. Thus, contrary to statements in the literature, there is no a priori need for an eastern boundary layer which exchanges mass with an ideal interior.

This concept of a weak solution is implicit in recent theories of the large-scale oceanic circulation. For example, in the continuously stratified, quasigeostrophic model developed by Rhines and Young, the solution is singular at the boundary between the moving pool of homogenized potential vorticity and the motionless shadow region. Analogous surfaces of discontinuity enable the models discussed in previous studies to satisfy eastern boundary conditions. The present study makes this assumption more explicit and shows how one particular dissipative mechanism (vertical density diffusion) heals the singularity.

## 1. Introduction

The thermocline equations [see (2.1) below] are a well known, and generally accepted, model for the large-scale, interior circulation of the ocean. However, despite thirty years of theoretical effort and some recent advances, there are still some unresolved questions about the well-posedness of the "ideal" (i.e., nondissipative) fluid model.

Specifically, Killworth (1983) has given a proof, see appendix A, that if the density at the eastern boundary varies smoothly with $z$ then the ideal fluid model has no solutions which satisfy a no-flux condition [$u(0, y, z) = 0$] at the eastern boundary ($x = 0$). If this is accepted then no-flux is not an appropriate boundary condition to apply to the ideal fluid equations. Instead one might argue, for instance, that there is a dissipative eastern boundary layer which accepts mass from the ideal fluid interior at one position and returns it at another. This was the philosophy adopted by Huang (1986), and it is implicit in earlier thermocline models (e.g. Needler, 1967, or Welander, 1971b).

On the other hand, there are solutions of the ideal fluid equations which are smoothly stratified on the eastern boundary and do satisfy a no-flux condition there. One such, taken from Pedlosky and Young (1982), is illustrated in Fig. 1. If these are accepted as valid then Killworth's theorem, while mathematically impeccable, is irrelevant because solutions of the ideal fluid equations violate its premises.

From a mathematical view, there is no contradiction here. Killworth's proof assumes that the density field is infinitely differentiable (see Appendix A) and the solution in Fig. 1, and others in Pedlosky and Young (1983), clearly violate this assumption. Because these solutions are not infinitely differentiable, we shall refer to them as "weak solutions". Are weak solutions physical in the present context? The conclusion reached here is that they are.

In summary, one might say there are two alternatives. If one requires that the solutions of the ideal problem be smooth (infinitely differentiable everywhere), then they cannot satisfy a no-flux condition at the eastern boundary. Alternatively, one can construct weak solutions and allow discontinuities in the density, or its derivatives, at certain initially unknown positions in the interior [e.g., the curve $z = -D(x, y)$ in Fig. 1] and satisfy a no-flux condition at the east. There are

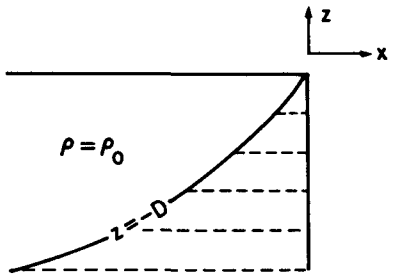


FIG. 1. A schematic density section in the subtropical gyre. The region above $z = -D(x, y)$ is fluid of uniform density $\rho_0$ injected from the Ekman layer. Below $z = -D$ the fluid is stratified and motionless. The dashed lines represent isopycnals. There is no flow through the eastern boundary.

examples of both choices in the literature. Most recently, Huang (1986) has made the first and Pedlosky and Young (1982) the second.

It is probably true that if one remains strictly within the *mathematical* framework of the ideal fluid model, it is impossible to say if either of the two alternatives above is *physically* preferable. If it could be shown that the ideal fluid equations are strictly hyperbolic, then discontinuities in the solutions would be expected and acceptable. Arguments along these lines are inconclusive (Huang, 1986).

The position taken here is that the ideal fluid model must be understood as the limiting case of a dissipative model. For example, if the density diffusivity, $\kappa$, is nonzero in (2.1e), then the density must be infinitely differentiable everywhere. Also, when $\kappa$ is nonzero, Killworth's proof does not generalize so one might expect that for a diffusive model a no-flux condition is possible. Indeed some specific solutions of the diffusive thermocline equations which have both of these desireable properties are exhibited below. Now as the limit $\kappa \to 0$ is taken, do either of these properties (smoothness and no-flux) survive?

We answer this question by showing as the diffusivity becomes small the solutions continue to satisfy the eastern no-flux boundary conditions, but also develop regions of rapid variation in the interior which can be clearly identified with surfaces of density discontinuity in the ideal limit. Thus, no-flux at the eastern boundary is a possible boundary condition for the ideal fluid model. And correspondingly surfaces of discontinuity in the interior are no cause for alarm.

This is not to say that eastern boundary layers which exchange mass with an interior flow do not exist. Cox and Bryan's (1984) simulation shows that they do. The issue is whether we fully understand the implications of assuming that the interior flow is ideal. Here we argue that if this is accepted as a working hypothesis then, contrary to the straightforward interpretation of Killworth's theorem, no mass flux at the east is certainly a possible boundary condition. And in the absence of an explicit model of the eastern boundary layer this is probably the best choice because it makes the mildest assumptions about the effects of unresolved physics.

Besides a discussion of eastern boundary conditions, this paper has some secondary goals. First we present a general class of similarity solutions which subsumes several earlier studies. Specifically the full thermocline equations, which have *three* independent variables ($x$, $y$, $z$), are reduced to a single partial differential equation with *two* independent variables [$y$, $\zeta \equiv -z/D(x, y)$]. Reduction of dimensionality is characteristic of similarity solutions, and the price paid for this simplification is that some of the boundary conditions of the higher dimensional system collapse onto one boundary condition for the lower dimensional system. In the present instance the eastern boundary ($x = 0$) and the abyssal region ($z = -\infty$) both correspond to $\zeta = \infty$. Consequently no motion at the eastern boundary implies no motion at great depths. We have thus eliminated the possibility of a barotropic component (Needler, 1967) and interaction with bottom topography. However, generality and realism is not our goal here. We regard these similarity solutions as local approximations of the flow near the eastern boundary. They indicate what physical assumptions about this region are acceptable in more complete models.

Another secondary goal is to present a numerical and analytic study of the similarity family found by Robinson and Welander (1963). These are in fact special cases (in which the partial differential equation in $y$ and $\zeta$ further reduces to an ordinary differential equation in $\zeta$) of the general family introduced above. Before attempting to solve this partial differential equation we must understand the special cases in which it becomes ordinary. Earlier investigators found isolated exact solutions of this complicated ordinary differential equation by dividing it into two parts, each of which vanished identically (e.g., see the review by Veronis, 1969). Here we abandon this search for exact solutions and confront the equation with a combination of numerical and asymptotic analysis. We believe this effort is worthwhile because Robinson and Welander's model

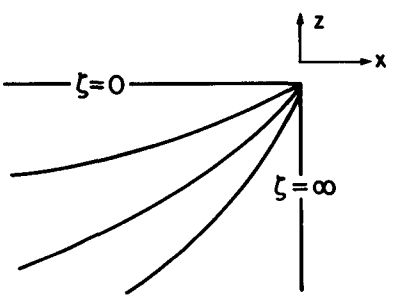


FIG. 2. Curves of constant $\zeta \equiv -z/D(x, y)$ in the $x$–$z$ plane (schematic). $\zeta = 0$ is the surface ($z = 0$, $x < 0$). Because $D \to 0$ as $x \to 0$ the curves $\zeta \gg 1$ are at once the eastern and abyssal region.

has some realistic features which the ad hoc exact solutions fail to capture. In particular, it was never entirely clear exactly what physical boundary conditions these exact solutions were meant to satisfy. But this is a failure of the exact solutions rather than the original model.

An example may make this clearer. The Blasius boundary layer on a flat plate (e.g., Batchelor, 1967) is calculated by numerically solving the two-point boundary value problem:

$$\left.\begin{aligned} &\tfrac{1}{2}ff''+f'''=0 \\ &f=f'=0 \quad \text{at} \quad \eta=0 \\ &f'\to 1 \quad \text{as} \quad \eta\to\infty \end{aligned}\right\}. \tag{1.1}$$

However, Eq. (1.1a) has some exact solutions (e.g., $f = -6/\eta$) which do not satisfy the appropriate boundary condition and have no obvious relationship to any physical problem. Isolating these does not help one solve (1.1) or understand its physical implications. Likewise, the failure of these exact solutions to correspond to any physical problem is not a criticism of (1.1) or the assumptions which led to it—it just means that the solution which satisfies the boundary conditions must be obtained numerically. And doing this is the final test of the similarity hypothesis used to obtain (1.1) in the first instance.

Robinson and Welander's (1963) family has an analogous structure; there is a complicated ordinary differential equation (fourth-order and nonlinear) and there are boundary conditions that essentially imply that the density is specified at the surface ($\zeta = 0$) and at the eastern boundary ($\zeta = \infty$). It may be possible to find exact solutions of the equation, but unless they also satisfy the boundary conditions they are unphysical. Unfortunately, solving the equation numerically is not easy; it is a two-point boundary value problem on the interval 0 to $\infty$ with two unknown initial values at each end. Further, there are singular solutions (poles) which appear spontaneously if there are slight errors in guessing the initial values. These complications are sufficient to defeat the shooting-Newton iteration rou-

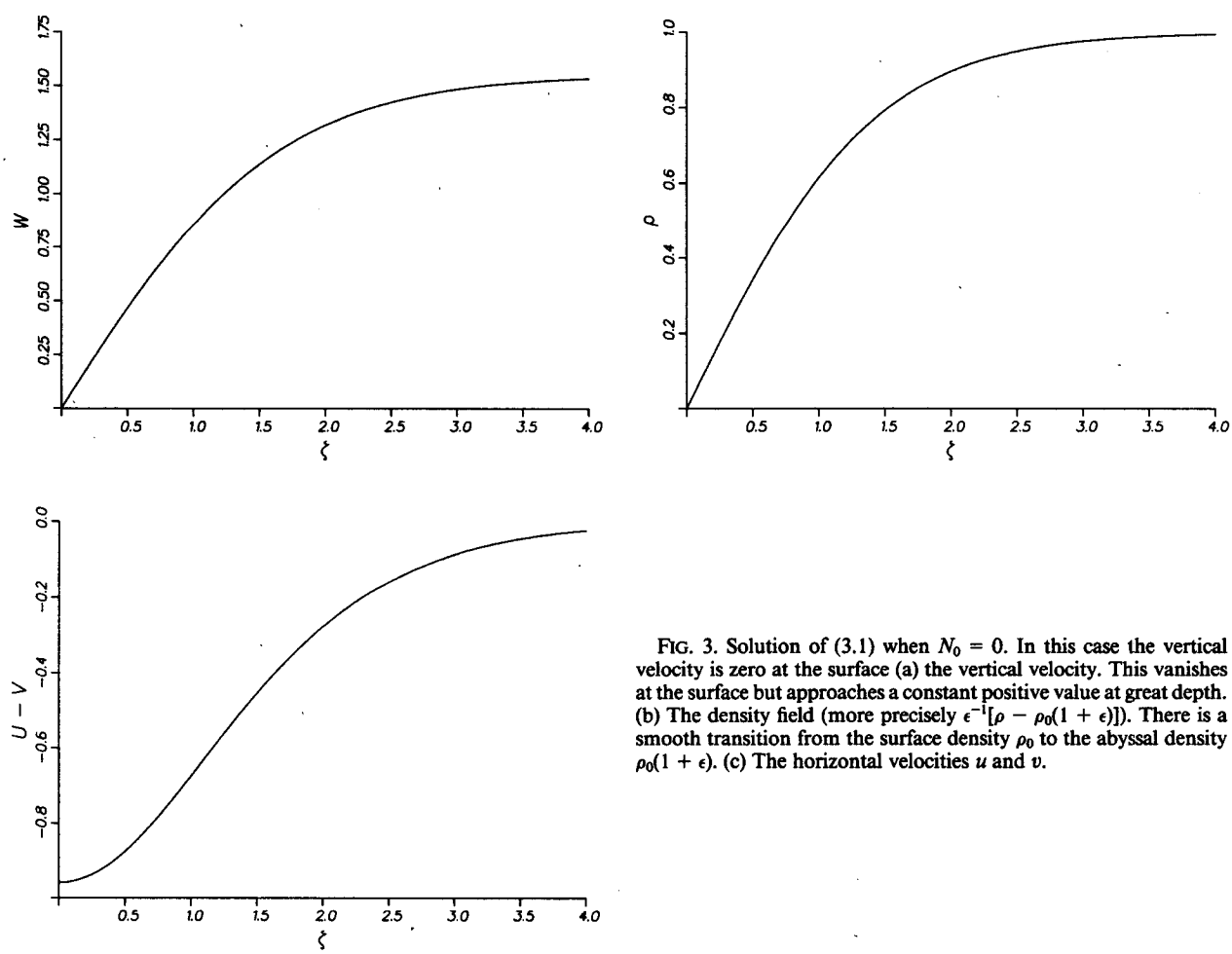


FIG. 3. Solution of (3.1) when $N_0 = 0$. In this case the vertical velocity is zero at the surface (a) the vertical velocity. This vanishes at the surface but approaches a constant positive value at great depth. (b) The density field (more precisely $\epsilon^{-1}[\rho - \rho_0(1 + \epsilon)]$). There is a smooth transition from the surface density $\rho_0$ to the abyssal density $\rho_0(1 + \epsilon)$. (c) The horizontal velocities $u$ and $v$.

tines available in the Nottingham Algorithms Group (NAG) library. A more sophisticated approach, using global approximation, was needed, and this is described in appendix B.

## 2. The thermocline equations and a family of solutions

In standard notation the thermocline equations are

$$\left.\begin{aligned} fu &= -p_y/\rho_0 \\ fv &= p_x/\rho_0 \\ 0 &= p_z + \rho g \\ u_x + v_y + w_z &= 0 \\ u\rho_x + v\rho_y + w\rho_z &= \kappa\rho_{zz} \end{aligned}\right\}. \tag{2.1}$$

This is the "$\beta$-plane" model:

$$f = \beta y. \tag{2.2}$$

The use of spherical coordinates introduces only notational changes. Some important, derived results used below are

$$\left.\begin{aligned} \beta v &= f w_z \\ f u_z &= g\rho_y/\rho_0 \\ f v_z &= -g\rho_x/\rho_0 \\ u q_x + v q_y + w q_z &= \kappa q_{zz} \end{aligned}\right\} \tag{2.3}$$

where $q = f\rho_z$ is the potential vorticity.

The arguments here are based on a "similarity" solution of (2.1). This solution is actually a special case of those found by Robinson and Welander (1963). However, we also show that Robinson and Welander's class of solutions is in turn subsumed by a still more general family.

This general family consists of solutions of (2.1) having the form

$$\begin{aligned} p &= -\rho_0 g z + \rho_0 g \epsilon D^{m+1} l^{-m} M_\zeta(\zeta, y) \\ \zeta &= -z/D(x, y) \end{aligned} \tag{2.4}$$

where $D$ is a function of $x$ and $y$ with dimensions of length, $\epsilon$ is dimensionless, and $l$ is a length scale. These external parameters are associated with the eastern

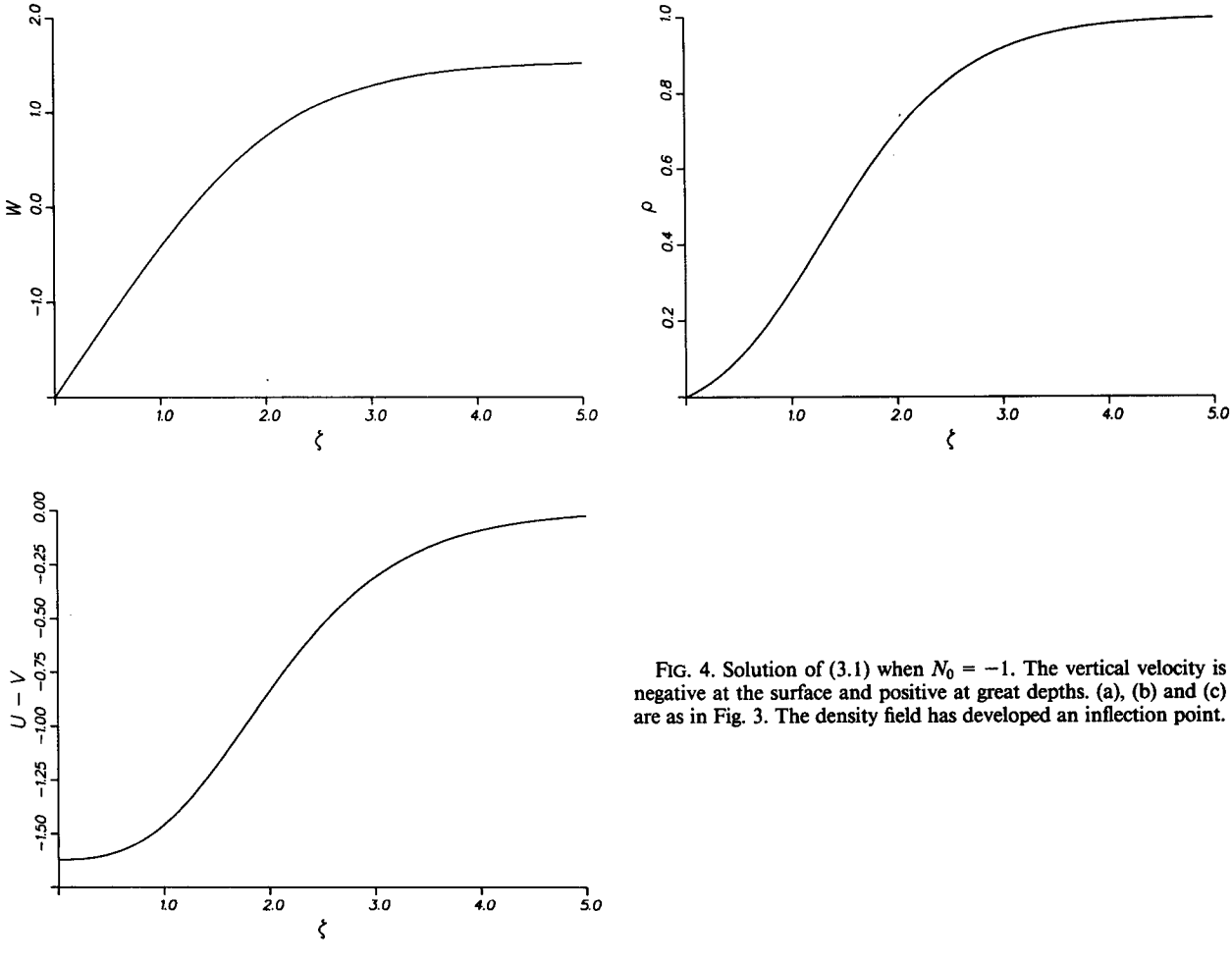


FIG. 4. Solution of (3.1) when $N_0 = -1$. The vertical velocity is negative at the surface and positive at great depths. (a), (b) and (c) are as in Fig. 3. The density field has developed an inflection point.

boundary condition (2.5). Substitution of (2.4) into (2.1) ultimately leads to a partial differential equation for $M$ as a function of $\zeta$ and $y$. Essentially $M$ is Welander's potential function. To recover Robinson and Welander's reduction, one substitutes $M(\zeta, y) = y^r Q(\zeta)$ and obtains an ordinary differential equation for $Q(\zeta)$ [essentially (32) in Robinson and Welander].

In (2.4) $\zeta$ is a similarity variable and, in anticipation of the calculation below, some curves of constant $\zeta$ in the $(x, z)$ plane are shown in Fig. 2. At this stage one should simply note that $D \to 0$ as $x \to 0$ so that the eastern boundary is $\zeta \to \infty$. The implication is that if the surface ($\zeta = 0$) density is a function of $y$, and the density at the eastern boundary only depends on $z$, then there is a discontinuity in the corner where the similarity variable is degenerate. The solutions here show how density diffusion smooths this discontinuity in the interior of the fluid. Thus, physically, we are investigating how diffusive thermocline dynamics smooths density discontinuities imposed by boundary conditions.

At the eastern boundary the density is of the form:

$$\rho = \rho_0\{1 + \epsilon(-z/l)^m\}, \quad m \geq 0. \tag{2.5}$$

Here $\epsilon$ and $l$ are introduced separately so that in the important special case $m = 0$, the density at great depths, and at the eastern boundary, is $\rho_0(1 + \epsilon)$. The density field in (2.5) will be referred to as the "resting stratification". Only a limited class of eastern density fields is admitted by the similarity solution (2.5). We can explicitly demonstrate that for this class of boundary conditions, density discontinuities arise in the ideal limit. Despite these restrictions we assert it as plausible that for arbitrary eastern density fields analogous discontinuities arise.

Note $\zeta \to \infty$ encompasses *two* boundary conditions (eastern and abyssal) in physical space. This "collapse" of two conditions in the three-dimensional $(x, y, z)$ space into one condition in the $(y, \zeta)$ space is typical of similarity solutions. If this did not happen it would be impossible for the lower dimensional system to satisfy all the boundary conditions of the higher one.

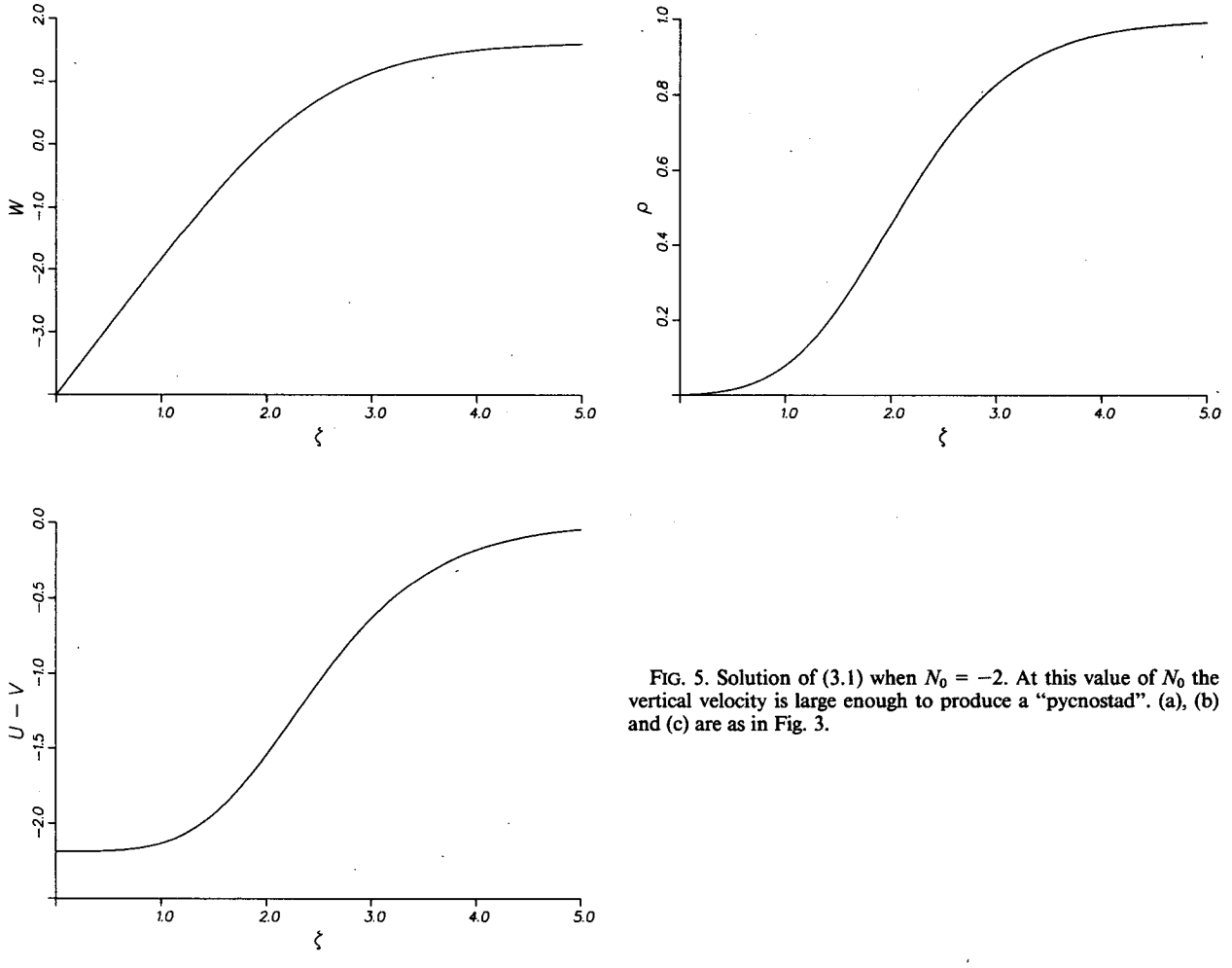


FIG. 5. Solution of (3.1) when $N_0 = -2$. At this value of $N_0$ the vertical velocity is large enough to produce a "pycnostad". (a), (b) and (c) are as in Fig. 3.

From (2.4) and the hydrostatic relation one can calculate the density:

$$\rho = \rho_0[1 + \epsilon(D/l)^m M_{\zeta\zeta}]. \tag{2.6}$$

If the above is to satisfy the eastern boundary condition, (2.5), then

$$M_{\zeta\zeta} \to +\zeta^m \quad \text{as} \quad \zeta \to \infty. \tag{2.7}$$

More precisely we require that the difference between $M_{\zeta\zeta}$ and $\zeta^m$ vanish as $\zeta \to \infty$. Generally this difference will vanish as some algebraic power of $\zeta$ (e.g., $\zeta^{-3}$). In special cases ($m = 0, 1$) it is exponentially small.

Once the form of $p$ has been specified, as in (2.4), there is some straightforward, tedious algebra required to calculate $u$, $v$ and $w$ from the equations of motion. The density conservation relation finally leads to a partial differential equation for $M$. Those not interested in the details of the substitution can skip forward to (2.12).

The horizontal velocities are given by the geostrophic balance:

$$\begin{aligned} fu &= -\epsilon g D_y (D/l)^m[(m+1)M_\zeta - \zeta M_{\zeta\zeta}] - \epsilon g D^{m+1} l^{-m} M_{\zeta y} \\ fv &= \epsilon g D_x (D/l)^m[(m+1)M_\zeta - \zeta M_{\zeta\zeta}]. \end{aligned} \tag{2.8}$$

The most direct way to calculate $w$ is from (2.3a):

$$w = -(\beta\epsilon g/f^2)(D/l)^m DD_x[(m+2)M - \zeta M_\zeta]. \tag{2.9}$$

To obtain an equation for $M$, substitute (2.6), (2.8) and (2.9) into (2.1e). Note the following intermediate step

$$\begin{aligned} fu\rho_x + fv\rho_y = \epsilon^2 g\rho_0 (D/l)^{2m} D_x\{\zeta[M_{\zeta y} M_{\zeta\zeta\zeta} - M_{\zeta\zeta y} M_{\zeta\zeta}] \\ + [(m+1)M_\zeta M_{\zeta\zeta y} - mM_{\zeta y} M_{\zeta\zeta}]\} \end{aligned}$$

which shows that if $M_y = 0$, then the horizontal advection vanishes. The result of the substitution is, finally

$$\begin{aligned} y\zeta[M_{\zeta\zeta\zeta} M_{\zeta y} - M_{\zeta\zeta} M_{\zeta\zeta y}] + y[(m+1)M_\zeta M_{\zeta\zeta y} \\ - mM_{\zeta y} M_{\zeta\zeta}] + [(m+2)M - \zeta M_\zeta] M_{\zeta\zeta\zeta} \\ = -\{-f^2 \kappa l^m / \beta\epsilon g D^{m+2} D_x\} M_{\zeta\zeta\zeta\zeta}. \end{aligned} \tag{2.10}$$

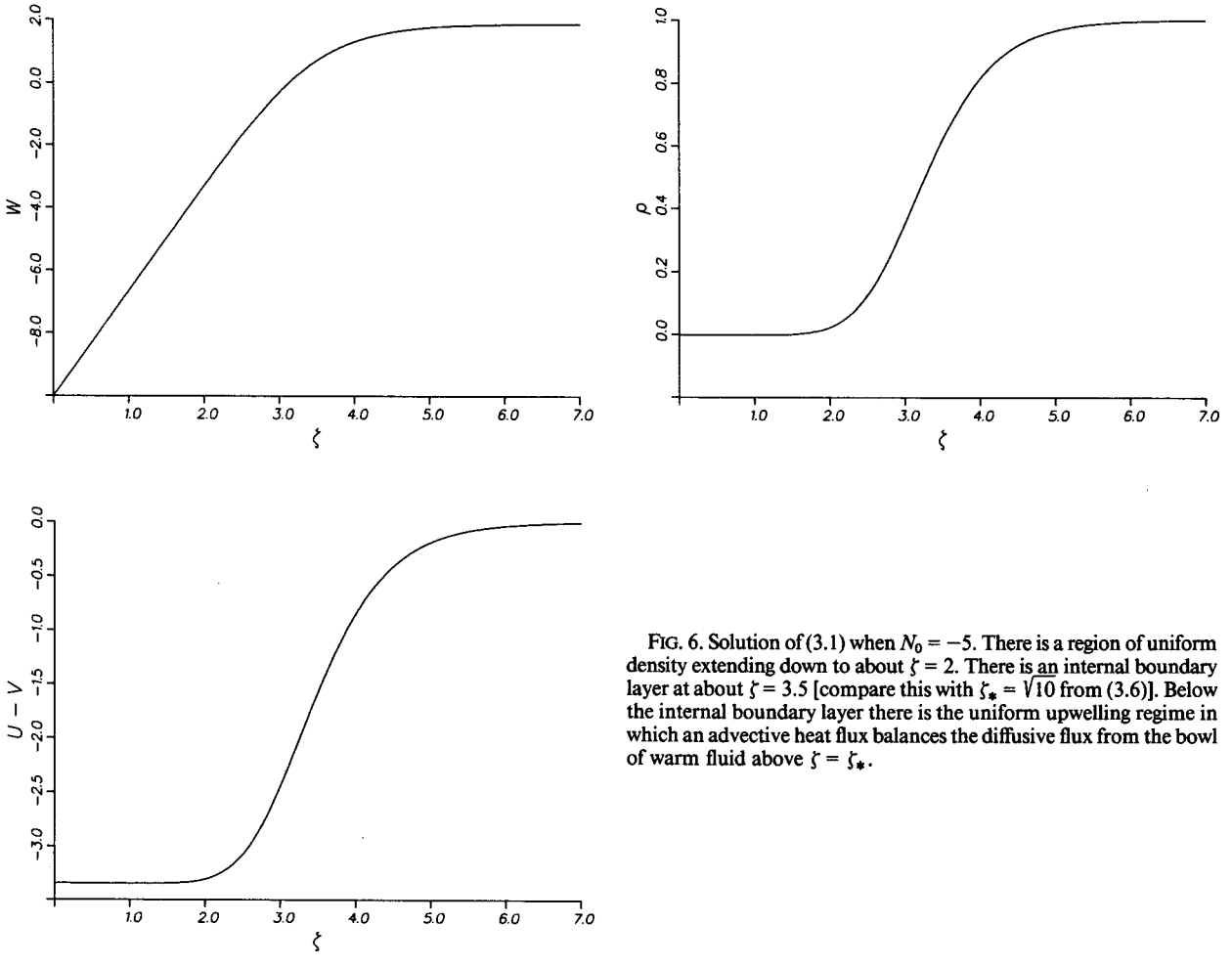


FIG. 6. Solution of (3.1) when $N_0 = -5$. There is a region of uniform density extending down to about $\zeta = 2$. There is an internal boundary layer at about $\zeta = 3.5$ [compare this with $\zeta_* = \sqrt{10}$ from (3.6)]. Below the internal boundary layer there is the uniform upwelling regime in which an advective heat flux balances the diffusive flux from the bowl of warm fluid above $\zeta = \zeta_*$.

TABLE 1. Summary of the numerical results for $m = 0$. The first three columns, together with $N_0'' = -1$, give the initial conditions needed to ensure $N'(\infty) = 0$. The constant value at infinity is given in column 4 and this should be compared with the estimate obtained from the asymptotic expansion (based on $N_0 \to -\infty$) in column 5.

| $N_0$ | $N_0'$ | $N_0'''$ | $N_\infty$ | $N_\infty$ from (3.7) |
|---|---|---|---|---|
| 0 | 0.9592 | 0.7102 | 0.774800 | |
| −1 | 1.6222 | 0.1268 | 0.768215 | |
| −2 | 2.1860 | 0.0112 | 0.817250 | |
| −4 | 3.0166 | 0.00 | 0.895292 | 0.913 |
| −5 | 3.3487 | 0.00 | 0.925716 | 0.937 |
| −6 | 3.6482 | 0.00 | 0.952678 | 0.960 |

Now because $M$ does not depend on $x$, the first term in curly brackets on the right hand side must be a function of $y$ alone, say:

$$-\beta\epsilon g D^{m+2} D_x / f^2 \kappa l^m = A(y)$$

or

$$D^{m+3} = (m+3)\{f^2\kappa l^m A(y)/\beta\epsilon g\}(-x). \quad (2.11)$$

With the above, (2.10) is

$$A(y)\{y\zeta[M_{\zeta\zeta\zeta}M_{\zeta y} - M_{\zeta\zeta}M_{\zeta\zeta y}] + y[(m+1)M_\zeta M_{\zeta\zeta y} - mM_{\zeta y}M_{\zeta\zeta}] + [(m+2)M - \zeta M_\zeta]M_{\zeta\zeta\zeta}\} = -M_{\zeta\zeta\zeta\zeta} \quad (2.12)$$

and this is the most general result for $M$. Various other reductions in the literature (e.g., Robinson and Stommel, 1959; Robinson and Welander, 1963; Luyten et al., 1983; Gill, 1985) are special cases of (2.10) and (2.12). These connections are explored in appendix C and sections 3 and 4.

Section 3 discusses in detail a special case of (2.12): $M_y = 0$. With this restriction $A(y)$ must be a constant, say 1, and (2.12) is

$$[(m+2)M - \zeta M_\zeta]M_{\zeta\zeta\zeta} = -M_{\zeta\zeta\zeta\zeta}. \quad (2.13)$$

As was noted above, if $M_y = 0$ then the horizontal advective terms vanish identically. Hence (2.13) is simply the vertical balance

$$w\rho_z = \kappa\rho_{zz}. \quad (2.14)$$

It is convenient to rewrite (2.13) by putting $M$ in the form

$$M(\zeta) = [\zeta^{m+2}/(m+1)(m+2)] + N(\zeta) \quad (2.15)$$

i.e., from (2.7) $N$ is the difference between $M$ and its asymptotic value. For $N$ one finds

$$[(m+2)N - \zeta N_\zeta][m\zeta^{m-1} + N_{\zeta\zeta\zeta}] = -m(m-1)\zeta^{m-2} - N_{\zeta\zeta\zeta\zeta} \quad (2.16)$$

and the boundary conditions on $N(\zeta)$ are

$$\left.\begin{aligned} N(0) &= N_0 \\ N''(0) &= 0 \quad \text{if} \quad m \neq 0 \\ N''(0) &= -1 \quad \text{if} \quad m = 0 \\ N'(\infty) &= 0 \end{aligned}\right\}. \quad (2.17)$$

Equations (2.8) and (2.9) give the velocity in terms of $M$. It is easily verified that $M$ can simply be replaced by $N$ in these results.

The first of (2.17) specifies the strength of the Ekman pumping at $z = 0$. In dimensional terms one has from (2.9) and (2.11)

$$w_0 \equiv w(x, y, 0) = (\kappa/D)(m+2)N_0 \quad (2.18)$$

so that as $N_0 \to -\infty$ with all other external boundaries fixed, we anticipate recovering the ideal fluid limit.

The second boundary condition in (2.17) is that the surface density is $\rho_0$. Specifically the density is given in terms of $N$ by

$$\rho = \rho_0[1 + \epsilon(-z/l)^m + \epsilon(D/l)^m N_{\zeta\zeta}] \quad (2.19)$$

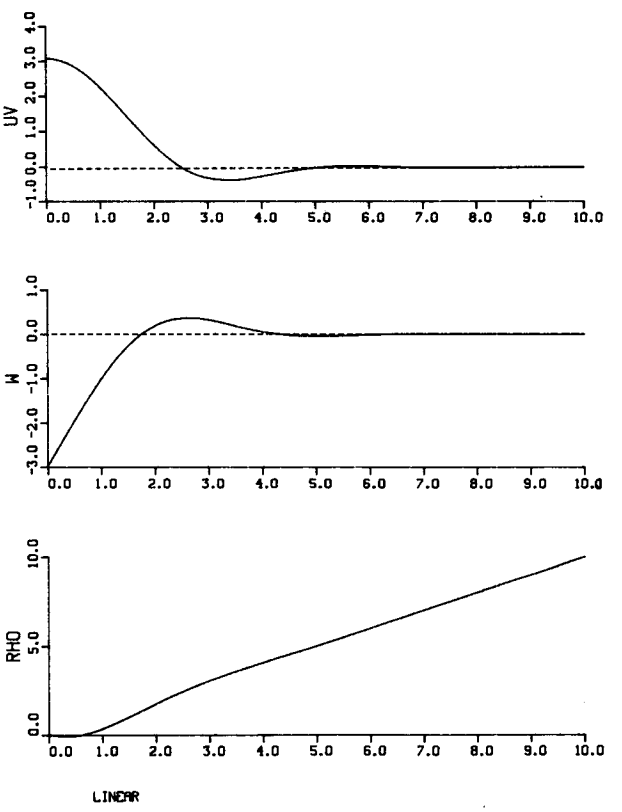


FIG. 7. The linear solution from (4.2). (a) The horizontal velocities (b) The vertical velocity (c) The density field, $\zeta + N_0 L\zeta\zeta$ with $N_0 = -1$. With this value of $N_0$ the linear theory has a slight density inversion when $\zeta < \frac{1}{2}$.

so that if the surface density is to be $\rho_0$, the case $m = 0$ must be distinguished. The third condition in (2.17) is that deep density field, and the density on the eastern boundary, is given by the resting stratification in (2.5). This condition also implies that the horizontal velocities in (2.8) also vanish at great depth. More precise statements about the asymptotic behavior of $N$ as $\zeta \to \infty$ are given in the next sections.

## 3. The case $m = 0$

We begin our discussion of (2.16) with the simplest, and perhaps the most realistic, special case. This is $m = 0$, and from (2.5) we see that the resting stratification in (2.5) is uniform. When the density is uniform on the eastern boundary, Killworth's argument is inapplicable [(A1) does not imply that $w = 0$] and so this calculation does not assist us in deciding between the two alternatives described in the introduction. Nonetheless it is worthwhile discussing $m = 0$ in some detail, both because of its intrinsic interest and because it is the simplest illustration of the mathematical techniques used to understand the general case.

It is interesting that the equation of motion when $m = 0$ [(3.1) below] is equivalent to the heuristic thermocline model of Robinson and Stommel (1959) and Stommel and Webster (1962). In these earlier models certain horizontal advective terms were arbitrarily neglected. The calculation in the previous section shows that when $M_y = 0$, they vanish identically. Thus, the quasi-vertical balance (2.14), which these earlier works assumed, is shown to be a consequence of the simplest boundary conditions: $\rho = \rho_0$ at the surface ($\zeta = 0$) and $\rho = \rho_0(1 + \epsilon)$ at the eastern boundary ($\zeta = \infty$).

Figures 3 through 6 show the numerical solution of

$$(2N - \zeta N_\zeta)N_{\zeta\zeta\zeta} = -N_{\zeta\zeta\zeta\zeta}$$
$$N(0) = N_0, N''(0) = -1, \quad N'(\infty) = 0 \qquad (3.1)$$

for various values of $N_0$. Of particular interest is the constant

$$N_\infty \equiv N(\infty). \qquad (3.2)$$

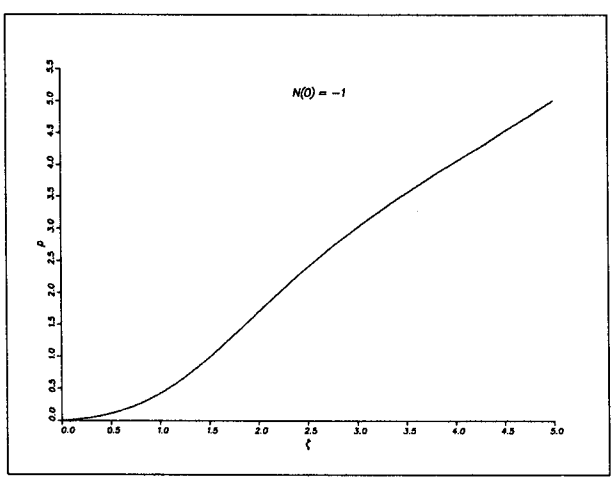


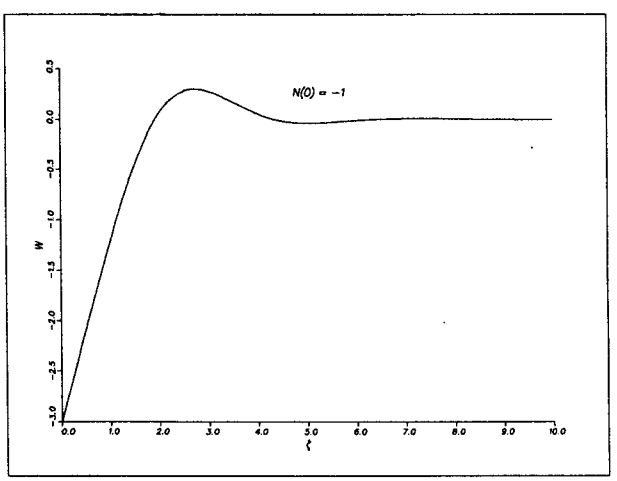


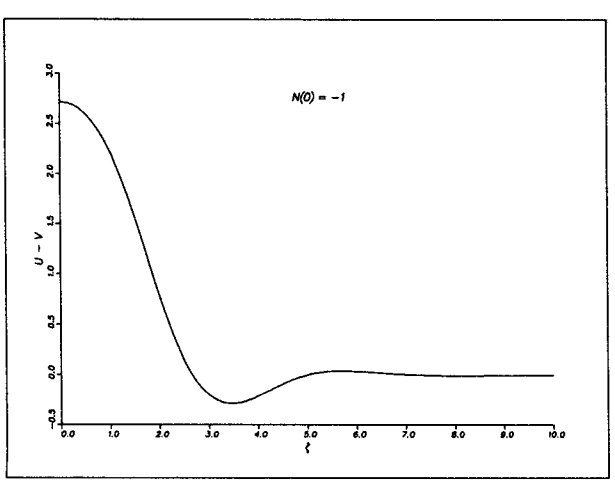


FIG. 8. The numerical solution of (4.1) with $N_0 = -1.0$. There is no density inversion in this full nonlinear solution. Also in contrast to the $m = 0$ solution in Figs. 3 through 6 the vertical velocity vanishes in the abyssal region.

From (2.9) it follows that the deep upwelling velocity is independent of $z$:

$$w_\infty = (\kappa/D)2N_\infty. \tag{3.3}$$

In Table 1 the results of calculations with several different values of $N_0$ are summarized. It follows from (2.14) that $\rho$ exponentially approaches its asymptotic value as $z \to -\infty$. This is a very familiar, classical picture (e.g., Robinson and Welander, 1963) in which uniform deep upwelling balances thermal diffusion from the surface.

The numerical solutions in Fig. 3 suggest that as $N_0 \to -\infty$ (i.e., the Ekman pumping becomes very strong), the solution develops an internal boundary layer at some position, say $\zeta_*$. We anticipate that the right-hand side of (3.1) is very small everywhere outside this boundary layer. In this case (3.1) reduces to a choice:

$$N_{\zeta\zeta\zeta} = 0$$

or

$$(2N - \zeta N_\zeta) = 0. \tag{3.4}$$

(At the moment these arguments are heuristic, but they suggest the scaling which ultimately formally justifies them.) Now the numerical solutions, and physical considerations, suggest that when $\zeta < \zeta_*$, (3.4a) applies (i.e., the density is vertically uniform and equal to its surface value). At $\zeta = \zeta_*$ there is an "exchange" and (3.4b) applies, i.e., the vertical velocity is zero (or no larger than the neglected term $N_{\zeta\zeta\zeta\zeta}$).

A simple calculation then gives

$$N = \begin{cases} -(\zeta - \zeta_*)^2/2, & \text{if } \zeta < \zeta_* \quad (3.5a) \\ 0, & \text{if } \zeta > \zeta_* \quad (3.5b) \end{cases}$$

where $\zeta_*$ is defined by

$$\zeta_* \equiv (-2N_0)^{1/2} \tag{3.6}$$

as an "outer" solution. This satisfies the boundary condition (3.1b) but has a discontinuous second derivative at $\zeta = \zeta_*$. Physically, this is a discontinuity in density. We expect to find an "inner" solution, in which diffusion is important, which effects a smooth transition between the "upper outer" solution (3.5a) and the "lower outer" (3.5b). This "inner" solution is an internal boundary layer located at $\zeta_*$. The transition is discussed in detail in appendix D using matched asymptotic expansions. The most important result is the following asymptotic ($\zeta_* \to \infty$) estimate of $N_\infty$:

$$N_\infty = 0.44\zeta_*^{1/2} + \frac{1}{2}\zeta_*^{-1} + O(\zeta_*^{-3/2}). \tag{3.7}$$

This is the correction to (3.5b) and from (3.3) it represents a deep upwelling velocity whose advective heat transport balances downward diffusion from the "bowl" of warm water injected by the Ekman pumping. In Table 1 the asymptotic prediction (3.7) is satisfactorily compared with the numerical solution of (3.1).

Some features of this asymptotic limit were anticipated by Welander's (1971a) scale analysis. He defined a "diffusive depth" by

$$d \equiv \kappa/|w_0| = D/\zeta_*^2 \tag{3.8}$$

and an "advective depth" by

$$a \equiv \zeta_* D. \tag{3.9}$$

Thus, $a(x, y)$ is the dimensional depth of the circulation in (3.5) and $d(x, y)$ was defined using $w_0$ in (2.18). As Welander noted, $D = a^{2/3}d^{1/3}$ is the vertical scale on which advection and diffusion can balance. In fact this is the depth of the circulation only when $N_0$, or equivalently $\zeta_*$, is order one. However, as $\zeta_*^3 = 1/\delta = a/d$ becomes large, we have shown that the depth of the circulation is $a$, i.e., most of the motion is confined to a layer of thickness "$a$" whose density reflects its origin at the surface. The detailed asymptotics above shows that this bowl of uniform fluid is bounded below by a diffusive, internal boundary layer of thickness $a^{1/2}d^{1/2}$. Heat diffuses out of the bowl, through the boundary layer, and into the abyssal region. This diffusive flux is balanced by a vertical upwelling which,

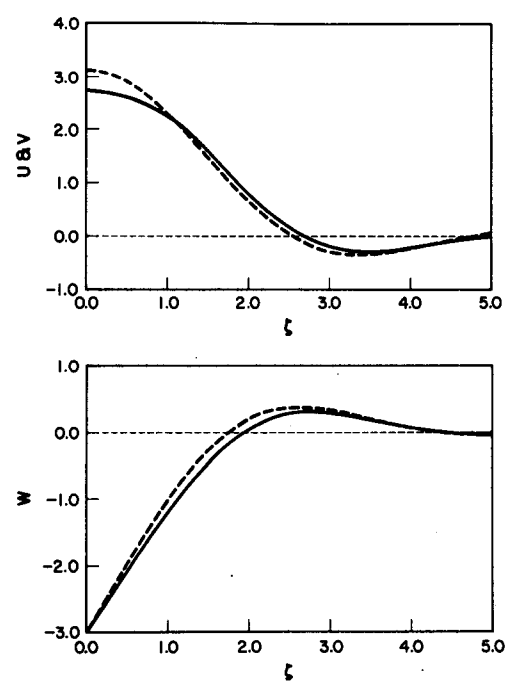


FIG. 9. A comparison of the velocities predicted by the linear theory with those of the nonlinear. Even though the linear theory predicts a density inversion when $N_0 = -1$ its velocities closely resemble those of the nonlinear solution. The linear solution is the dashed curve and the nonlinear the solid curve.

in the almost ideal limit ($a/d \gg 1$), is related to the surface Ekman pumping by

$$w_\infty = -0.88(d/a)^{1/2} w_0. \tag{3.10}$$

## 4. The case $m = 1$

Now consider $m = 1$. In this case the density of fluid at the eastern boundary increases linearly at depth—see (2.5). This is also the stratification in the abyss, below the influence of surface conditions. The equation of motion, (2.16), and the associated boundary conditions are

$$(3N - \zeta N_\zeta)\{1 + N_{\zeta\zeta\zeta}\} = -N_{\zeta\zeta\zeta\zeta}$$
$$N(0) = N_0, \quad N''(0) = 0, \quad N(\infty) = 0. \tag{4.1}$$

A simple analysis of (4.1a) shows that, if $\zeta N_\zeta \to 0$ as $\zeta \to \infty$, then $N$ must also vanish. Thus, in (4.1b) we require that $N(\infty) = 0$ rather than some unspecified constant. Consequently the vertical velocity vanishes at great depth (in fact exponentially quickly), and this implies that the advective flux of heat also vanishes in the abyss. The conclusion is that the constant abyssal density gradient is maintained by a purely diffusive, nondivergent, downwards heat flux. It must be imagined that this flux is ultimately absorbed at great depths by some unspecified, nonintrusive mechanism. This is different from, and more artificial than, the previous case in which the deep advective and diffusive fluxes cancelled so that there was not net flux into or out of the abyss. Global heat fluxes are discussed in more detial in section 6 and the Conclusion.

One important consequence of this difference is that when $N_0$ is small, (4.1) can be linearized. Physically, one is supposing that the surface forcing is so weak that the resting stratification is almost undisturbed. This cannot be done with (3.1)—there is nothing to linearize "about".

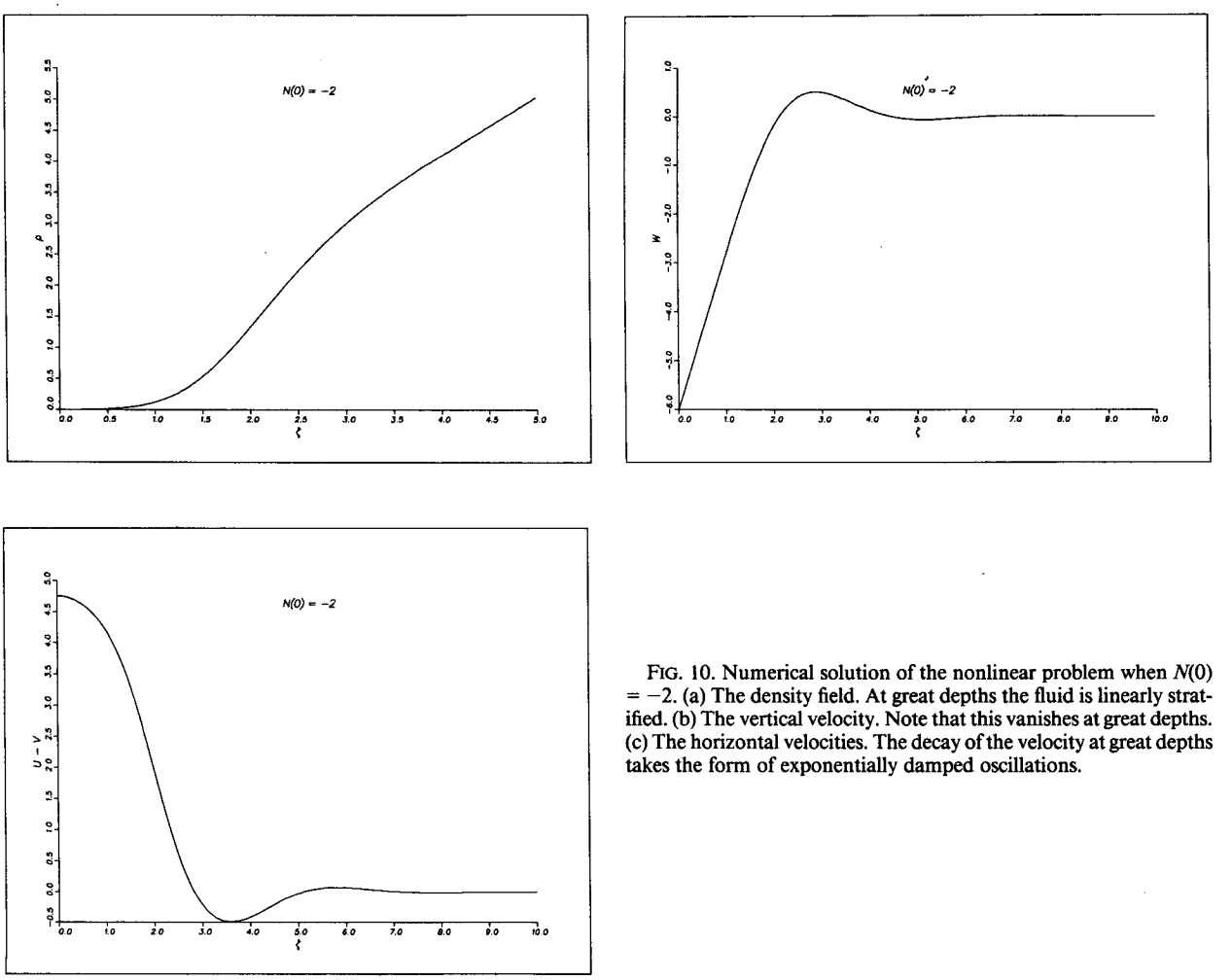


FIG. 10. Numerical solution of the nonlinear problem when $N(0) = -2$. (a) The density field. At great depths the fluid is linearly stratified. (b) The vertical velocity. Note that this vanishes at great depths. (c) The horizontal velocities. The decay of the velocity at great depths takes the form of exponentially damped oscillations.

The linearized problem is

$$3L - \zeta L_\zeta = -L_{\zeta\zeta\zeta}$$
$$L(0) = 1, \quad L''(0) = 0, \quad L(\infty) = 0 \qquad (4.2)$$

where $N = N_0 L$ and $N_0 \ll 1$. The above is essentially the diffusive thermocline model discussed by Gill (1985). The formal apparatus required to solve (4.2) was developed by Gill and Smith (1970). Figure 7 shows the solution of (4.2) obtained using these results. There is a slight density inversion because we have taken $N_0 = -1$ and used the linearized solution from (4.2). Apparently this value of $N$ is so large that the linear theory incorrectly predicts a density inversion. The nonlinear solution of (4.1) with $N_0 = -1$ is shown in Fig. 8, and there is no density inversion. However, the linear solution does respectably predict the velocities: Fig. 9 compares the linear prediction with the nonlinear solution.

Figures 10 and 11 show the solution with larger values of $|N_0|$. In Fig. 11, where $N_0$ is $-10$, there is a large region of fluid with uniform density $\rho_0$ which originated at the surface. The bowl is bounded below at about $\zeta = 3.5$ by a region of rapid variation (an internal boundary layer). At still greater depths there is the resting stratification in which the density increases linearly. It is clear that as $|N_0|$ becomes larger, the bowl of uniform fluid becomes deeper and the boundary layer "sharper". In the ideal limit the boundary layer has vanishing thickness and the density discontinuously changes from $\rho_0$ to the resting stratification. Throughout this limiting process the no-flux condition at the eastern boundary is satisfied.

The conclusion is that the ideal fluid equations have "weak" (i.e. discontinuous) solutions which can be understood as the singular limit of a dissipative model. In less artificial problems, where the Ekman pumping and surface density are independently specified and no similarity solutions exist, we may expect analogous behavior. And this is an important ingredient of the circulation theories given by Rhines and Young (1982), Luyten et al. (1983) and Pedlosky and Young (1983). In all of these theories there are domain boundaries that separate different flow regimes (e.g., Figs. 4, 9 and

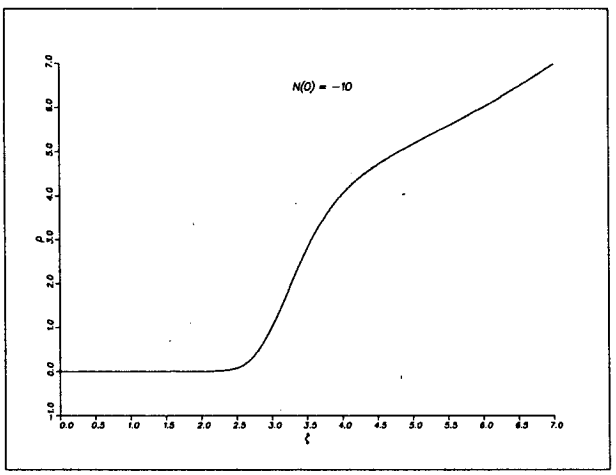


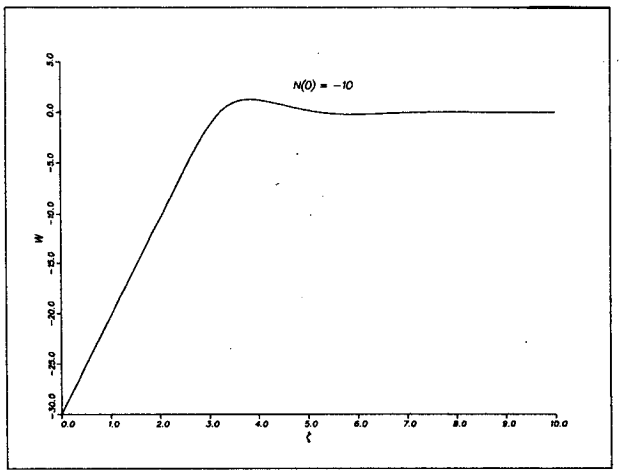


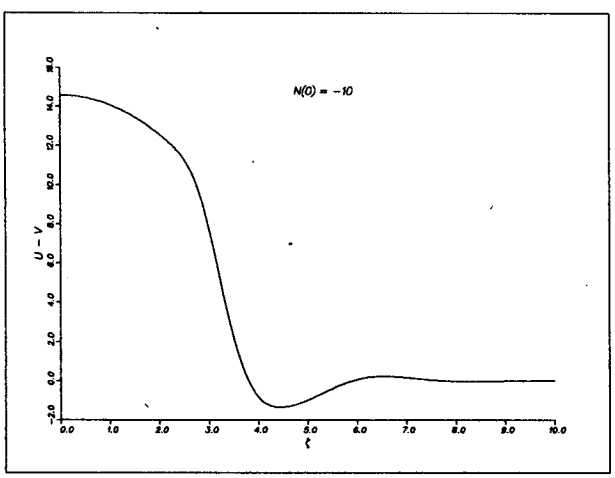


FIG. 11. Numerical solution of the nonlinear problem when $N(0) = -10$. In this case the vertical velocity is large enough to create a "pycnostad" of density $\rho_0$ which extends down to about $\zeta = 2.7$. The vertical velocity is a linear function of depth in this region. The pycnostad is bounded below by an internal boundary layer at about $\zeta = 3.6$ [compare this with $\zeta_* = 30^{1/3} = 3.1$ from (4.4).] At still greater depths is found linearly stratified motionless fluid.

TABLE 2. Summary of the numerical results for $m = 1$. These three numbers, together with $N_0'' = 0$, are the initial conditions needed to ensure that $N(\infty) = 0$. Row 1 is the linear solution (Gill, 1985), in which $N_0$ is equal to some small number, $a$, and the other starting conditions are proportional to this.

| $N_0$ | $N_0'$ | $N_0'''$ |
|---|---|---|
| $a \ll 1$ | $(-1.037051)a$ | $(1.838125)a$ |
| $-1$ | 0.90508 | $-0.892$ |
| $-2$ | 1.5854 | $-0.995$ |
| $-4$ | 2.6126 | $-1.00$ |
| $-6$ | 3.4483 | $-1.00$ |
| $-10$ | 4.8605 | $-1.00$ |

10 in Pedlosky and Young). At these initially unknown boundaries the solution is not analytic and the assertion is that a slight amount of dissipation smooths these discontinuities into internal boundary layers. Calculation of the detailed local structure of the boundary layer may be quite involved (e.g., the analysis in section 3) and of course requires a specific model for the dissipation (e.g., $\kappa\rho_{zz}$). However, the *location* of the boundary layers (at least to zero order) and their important global role in satisfying the boundary conditions can be simply understood from the ideal fluid model.

For example, consider (4.1) and suppose that $|N_0| \gg 1$. As in section 3 we argue that in most of the flow the diffusive term, $N_{\zeta\zeta\zeta\zeta}$, is small. Consequently, outside the boundary layers,

$$N_{\zeta\zeta\zeta} + 1 = 0. \tag{4.3}$$

The solution of the above which satisfies the boundary conditions is

$$N = \left\{ \begin{array}{ll} -(\zeta - \zeta_*)^2(\zeta + 2\zeta_*)/6, & \text{if } \zeta < \zeta_* \\ 0, & \text{if } \zeta > \zeta_* \end{array} \right\}, \quad \zeta_* = (-3N_0)^{1/3}. \tag{4.4}$$

The outer solution above is discontinuous at $\zeta = \zeta_*$. This is the *location* of the internal boundary layer. For example, when $N_0 = -10$, $\zeta_* = 3.1$, which compares favorably with the location of the region of rapid variation in Fig. 11.

To aid visualization in physical space, we have plotted a zonal density section in Fig. 12. In this figure $N_0 = -10$, and there is a large bowl of uniform density injected from the surface. The dashed curve is $\zeta = \zeta_*$, i.e., the prediction from (4.4c) of the location of the transition from uniform to linearly stratified fluid. The gentle undulations of the deep isopycnals are produced by the oscillatory decay of Gill and Smith's (1970) linear solutions. (Their analysis strictly applies in the deep fluid where the isopycnals are displaced only slightly from their resting positions.) This figure makes it clear that the addition of a small amount of vertical density diffusivity produces smooth fields that satisfy no-flux boundary conditions at the east. Also clearly indicated is the internal boundary layer which in the ideal limit is a discontinuity.

A detailed asymptotic analysis of the internal boundary layer at $\zeta_*$ boundary layer might now proceed along the lines of that in section 3. Prompted by human fatigability we do not undertake this chore, but instead remain content with the numerical solutions in Figs. 8, 10, 11 and 12, and the outer solution in (4.4). Finally, Table 2 provides the extra initial conditions needed to solve (4.1) numerically.

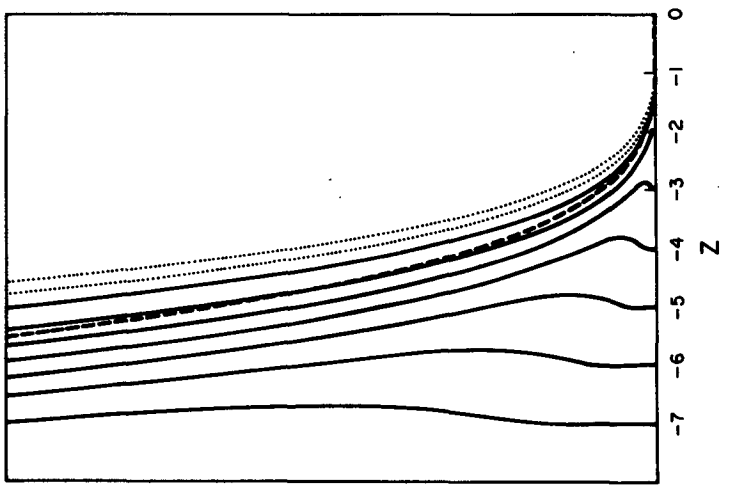


FIG. 12. A zonal density section (i.e., $Z + DN_{ff}$ with $D^4 \propto x$) from (2.11) when $N_0 = -10$. The horizontal units are arbitrary. The solid curves are isopycnals at equal intervals, say $\delta\rho = 1$. Thus the linear stratification on the eastern boundary is apparent. To emphasize the rapid density variation we've added two extra isopycnals (the dotted curves) which intersect the eastern boundary at $z = -\frac{1}{4}$ and $z = -\frac{1}{2}$. The dashed curve is $\zeta = \zeta_*$, i.e. the location of the internal boundary layer or from ideal fluid theory, the position of the density discontinuity.

## 5. The general case and some remarks on global balances

The similarity solutions discussed in the previous sections are not intended as global solutions. Their scope is much more modest; they illustrate how vertical diffusion smooths the density discontinuities produced by Ekman pumping, which injects light fluid into a sluggish abyssal region. This is shown in Fig. 12 where the deep isopycnals are nearly flat until they strike the intruding bowl of warm surface water.

But many central issues have been ignored. For instance, what determines the resting stratification (2.5)? The present family of similarity solutions assumes this is given at the outset. This assumption hides some important, and perhaps unrealistic, assertions about the global heat and mass fluxes required to establish this resting stratification.

This is apparent if we examine the asymptotic (i.e. $\zeta \to \infty$) behavior of $N$ in (2.16). This can be done linearly using

$$m\zeta^{m-1} \gg N_{\zeta\zeta\zeta} \quad \text{and} \quad m(m-1)\zeta^{m-2} \gg N_{\zeta\zeta\zeta\zeta}. \tag{5.1}$$

(Clearly $m$ cannot be equal to 0 or 1.) This calculation is straightforward, but it is physically more transparent to note that from (2.5) and (2.14) one can also calculate $w$ as $z \to -\infty$:

$$w \sim +\kappa(m-1)/z \tag{5.2}$$

provided $m \neq 0, 1$. A more careful analysis of (2.16) shows that the error in the above is $O(z^{-2})$, i.e., when $m \neq 0$ or 1, the velocities decay algebraically as $z \to -\infty$.

One can also calculate the deep heat flux associated with the resting stratification. Defining

$$\theta \equiv (\rho_0 - \rho)/\rho_0$$

the heat flux is proportional to

$$F \equiv w\theta - \kappa\theta_z$$
$$= -\epsilon\kappa(-z)^{m-1}/l \tag{5.3}$$

i.e. if $m = 1$, the heat flux is constant.

As Tziperman (1985) has recently emphasized, a steady state requires that the integrated interior mass and heat fluxes in (5.2) and (5.3) be balanced by equal and opposite net fluxes elsewhere. Presumably these fluxes are associated with penetrative deep-water formation in marginal seas. The power law family in (2.5) requires that these processes produce the net fluxes given by (5.2) and (5.3). This may not be realistic, e.g., if $m$ is greater than one, then (5.2) gives *negative* deep vertical velocities. Given the arbitrariness of these assumptions, we have not attempted a detailed investigation of the general case, $m \neq 0$ or 1.

These cautionary remarks emphasize that the similarity solutions lack some very important physics. They are unable to help us understand how the deep density field is maintained by arbitrarily specified mass and buoyancy sources (for which see Tziperman, 1985). In the present study they are best thought of as local solutions in the neighborhood of the eastern boundary. As such they illustrate the nonlinear transition between two different flow regimes and provide some clues as to what physical assumptions are acceptable in more ambitious, global models.

## 6. Conclusion

Solutions of the ideal fluid thermocline model that satisfy no-flux eastern boundary conditions must be singular (i.e., nondifferentiable) in the interior. It has been shown here that these "weak solutions" can be understood as the limiting case of a dissipative model.

Specifically, if vertical density diffusion is used as dissipation, then there are solutions that are both smooth and satisfy no-flux boundary conditions. As the diffusivity becomes small, or equivalently the Ekman pumping becomes large, the flow develops internal boundary layers which effect an abrupt transition between fluid of two different densities. In the singular limit, when the diffusion vanishes identically, these internal boundary layers are surfaces at which the density is discontinuous. Throughout this limiting process the flow continues to satisfy a no-flux boundary condition at the east.

We emphasize that this conclusion may depend on the choice of dissipative mechanism. If we used horizontal rather than vertical diffusion, the boundary layers *might* shift to the eastern wall. In fact, there is some evidence of this in the Cox and Bryan's (1984) numerical simulation. Their Figs. 2 and 5 show flow into and out of an eastern boundary layer. However, the velocities are much weaker than those in the interior except in small pockets near the northern and southern boundaries of the basin.

The one theoretical conclusion we can unequivocally draw is that there are physically sensible, nondifferentiable solutions of the ideal fluid thermocline equations ("weak solutions"). In other contexts (e.g., gas dynamics) the concept of weak solutions, and the recognition that the singularity is associated with the failure of some physical idealization (e.g., no dissipation), is familiar. The recent circulation theories of Rhines and Young (1982) and Luyten et al. (1983) have implicitly introduced this idea into thermocline theory. The present article has attempted to make the assumptions in these earlier studies both more explicit and more palatable.

*Acknowledgments.* This research was supported by the National Science Foundation under grants OCE-8421074 (WRY) and OCE-8515702 (GRI). We thank Charmaine King and Dorothy Frank for their assistance in preparing this manuscript.

APPENDIX A

## Killworth's Theorem

Killworth's theorem states that the only solution of the ideal fluid equations that satisfies

(i) $\rho_z(0, y, z) \neq 0$, i.e., the fluid at the eastern boundary is stratified;
(ii) $u(0, y, z) = 0$, i.e., no mass flux through the eastern boundary;
(iii) All derivative of $\rho$ exist everywhere

is the trivial solution $\mathbf{u}(x, y, z) = 0$.

Begin by noting that if $u = 0$ at $x = 0$, then from thermal wind, $\rho_y$ must also be zero. Then the density conservation equation reduces to

$$w\rho_z = 0. \tag{A1}$$

Because of (i) it follows that $w = 0$ at the eastern boundary. However, $\beta v = fw_z$ shows that $v$ is then also zero. Again because of thermal wind, it follows that $\rho_x$ is zero at the eastern boundary. Now if we differentiate (2.1e) with respect to $x$ and evaluate the resulting expression at $x = 0$, we find $w_x = 0$ on the eastern boundary. Again using the vertical vorticity equation and the thermal wind we find $\rho_{xx} = 0$. This process of taking $x$ derivatives of the density equation can be continued indefinitely, and at the $n$th stage the conclusion is that $\partial^n\rho/\partial x^n$ is zero. Hence, if $\rho$ is infinitely differentiable it must be equal to its value at the eastern boundary everywhere. Thus, the isopycnals are flat and the fluid is motionless. (In fact, even this conclusion needs qualification. For instance, the function $e^{-1/x^2}$ is infinitely differentiable and all its derivatives vanish at the origin, yet it is nonzero. Perhaps one should say that if (i), (ii) and (iii) above are satisfied, then the only "nonpathological" solution is $\mathbf{u} = 0$.)

APPENDIX B

## Numerical Methods

Several factors mitigate against the use of standard shooting methods for the nonlinear boundary value problems solved here. First, the problem requires a two-parameter shoot for unknown constants at the origin, and second, the occurrence of spontaneous singularities in the form of first-order poles poses a problem of severe numerical instability, indeed, only as the values of both parameters are accurately established does the pole recede to infinity. (The nature of the difficulties encountered here is quite similar to those found in a nonlinear boundary value problem discussed by Ierley and Ruehr, 1985, and a more complete discussion appears there.) The computation time required to find a solution of given accuracy is substantially diminished by the use of spectral methods, and the global character of the solution permits a simple application of the boundary conditions as $\xi \to \infty$, obviating the need for an ad hoc heuristic approach tailored to the numerical instabilities of the conventional shooting approach. The drawback of this approach lies in the relatively greater programming time required, and, to a degree, in the difficulty of adapting the program to minor changes in the problem.

A spectral representation of the solution is

$$f(\xi) = \sum_{n=0}^{K} f_n T_n(z(\xi)) \tag{B1}$$

where

$$z(\xi) = \frac{\alpha\xi - 1}{\alpha\xi + 1}.$$

Here $T_n$ is the $n$th Chebyshev polynomial. The "mapping parameter" $\alpha$ is adjusted so that the Chebyshev resolution is evenly distributed. With this variable change, (3.1) becomes

$$\left(\frac{(z-1)^4}{16}D^4 + \frac{3(z-1)^3}{4}D^3 + \frac{9(z-1)^2}{4}D^2 + \frac{3(z-1)}{2}D\right)f = \left(\frac{2f}{\alpha} + \frac{(z^2-1)}{2}Df\right)\left(\frac{(z-1)^2}{8}D^3 + \frac{3(z-1)}{4}D^2 + \frac{3}{4}D\right)f \tag{B2}$$

where the boundary conditions are:

$$\left.\begin{aligned} f(-1) &= 0 \\ f''(-1) - f'(-1) &= 0 \end{aligned}\right\} \tag{B3}$$

and $D$ denotes a $z$ derivative. An analogous equation for $m = 1$ can be derived. Imposing $f'(\infty) = 0$ is a little tricky because

$$\frac{df}{d\xi} = \frac{df}{dz}\frac{dz}{d\xi}$$

and $dz/d\xi$ tends to zero as $\xi \to \infty$. However, because we expect $df/d\xi$ to vanish exponentially rather than simply algebraically, we can still impose

$$\left.\frac{df}{dz}\right|_{\xi=1} = 0$$

which is easily implemented. For more general $m$, $f$ will decay only algebraically at $\infty$ and more care is required in the solution, but in any case the problem ought then to be reformulated with a decomposition other than that given in the body of the paper which introduces artificial singularities at the origin. It is perhaps best then to solve directly for $M$ imposing a condition on the asymptotic growth.

The strategy is now to determine the $f_m$ in (B1) by substituting this representation into (B2) and solving the resulting $K$th order system using Newton's method. In the examples presented here $K = 41$.

The solution for $m = 0$ poses the problem of finding a suitable initial guess for Newton's method because there is no linearization of the problem. To handle this, the problem

$$Lf = Nf$$

where $L$ represents the linear (diffusive) term, and $N$ the nonlinear terms, is written as a time dependent problem:

$$(\partial_t + 1)Lf = Nf$$

whose solution is evolved several hundred steps until reasonably equilibrated, and the output then used as an initial guess in Newton's method, which converges in three or four steps. This approach works acceptably for values of $N_0 \geq -6$, but instabilities observed in both the time dependent problem and Newton's method for values of $N_0$ smaller than this have not been satisfactorily resolved. For $m = 1$, solution of the related linear problem provides an adequate starting guess for Newton's method for all values of $N_0$ attempted.

After these rather complex methods, the solution of (3.15) is pleasantly straightforward. Define

$$\Omega_0' = \Lambda$$

$$\Lambda' = \Gamma. \tag{B4}$$

Then (3.15a) is

$$\Gamma' = -\Omega_0\Gamma. \tag{B5}$$

Equations (B4) and (B5) are equivalent to the original equation. Now use $\Lambda$ as a new independent variable. After some rearrangement:

$$\Gamma\frac{d^2\Gamma}{d\Lambda^2} = -\Lambda \tag{B6}$$

and a little thought shows that the boundary conditions, (3.15b), are

$$\Gamma = 0 \quad \text{at} \quad \Lambda = 0$$

$$\Gamma = 0 \quad \text{at} \quad \Lambda = 1. \tag{B7}$$

The first of these corresponds to $\eta = \infty$ in (3.15) while the second is $\eta = -\infty$. The unknown constant $c$ in (3.16) is the shooting parameter $d\Gamma(0)/d\Lambda$ required to ensure that $\Gamma(1) = 0$.

We observe that (B6) is unchanged by the transformation:

$$\Gamma \equiv k^3\Gamma_1, \quad \Lambda \equiv k^2\Lambda_1 \tag{B8}$$

numerically solve the *initial* value problem

$$\Gamma_1\frac{d^2\Gamma_1}{d\Lambda_1^2} = -\Lambda_1$$

$$\Gamma_1(0) = 0, \quad \frac{d\Gamma_1(0)}{d\Lambda_1} = 1$$

and find that $\Gamma_1(1.3039059221) = 0$. From (B8) this zero will be at $\Lambda = 1$ if $(1.3039)k^2 = 1$ or $k = 0.87574$ and this is also $d\Gamma(0)/d\Lambda$. Thus the unknown constant $c$ in (3.16) is calculated without trial-and-error shooting.

## APPENDIX C

### Connections with Earlier Solutions

One of the secondary goals of this paper was to present a new class of similarity solutions. For this class the *partial* differential equations in $(x, y, z)$ are reduced to a single partial differential equation in $y$ and $\zeta$ [see (2.12)]. In much of the earlier work an *ordinary* differential in the similarity variable was the goal (e.g., Robinson and Welander, 1963). While less general than the present approach this has the primary virtue of simplicity. Indeed the detailed calculations in the present article have been confined to the case in which (2.12) reduces to an ordinary differential equation. Further, we show below that our analysis has certainly not exhausted the instances in which this additional reduction of (2.12) is possible. The purpose of this appendix is to unify the various results in the literature and indicate those that are special cases of (2.12).

First consider (2.10). At this stage of the development $D$ has not been chosen to eliminate the $x$-dependence. In fact, we note that if $\kappa \equiv 0$, then the $x$-dependent term on the right-hand side vanishes! The implication is that for an ideal fluid problem, $D(x, y)$ can be selected to satisfy another boundary condition. Suppose for instance that $m = 0$. Then from (2.6) we have a boundary condition for $M$ at $\zeta = 0$.

$$\rho(x, y, 0) = \rho_0[1 + \epsilon M_{\zeta\zeta}(0, y)] \tag{C1}$$

i.e., the surface density can be an arbitrary function of $y$. Now from (2.9) at $\zeta = 0$

$$w(x, y, 0) = -(\beta\epsilon g/f^2)2DD_xM(0, y) \tag{C2}$$

so that by selecting $D(x, y)$ and $M(0, y)$ an arbitrary pattern of Ekman pumping can be accommodated. The freedom to satisfy these two surface boundary conditions independently depends crucially on the assumption that $\kappa = 0$. Otherwise one is forced to choose $D$ as in (2.11), and consequently from (2.18) the pattern of Ekman pumping is determined. Investigation of this particular simplification of the ideal fluid thermocline would take us too far afield. For the present we speculate that this may be a route to a continuously stratified model of the ventilated thermocline. Indeed Luyten et al.'s (1983) solution for the density field also has the form (2.6) with $m = 0$ if the depth of their first moving layer at the eastern boundary ($H_0$ in their notation) is zero.

Our present concern is not ideal fluid models but rather the diffusive case in which the choice of $D$ is dictated by (2.11). In this instance $M$ must be found by solving the rather complicated Eq. (2.12). However, this equation simplifies greatly if we look for solutions of the form

$$M(y, \zeta) = (y/a)^rG(\zeta), \quad A(y) = (y/a)^{-r} \tag{C3}$$

where $a$ has the dimensions of length. With the above the ordinary differential equation for $G$ is

$$r\zeta(G'G''' - G''^2) + rG'G'' + [(m+2)G - \zeta G']G''' = -G^{iv} \tag{C4}$$

where the dash is a $\zeta$-derivative. The above is essentially Eq. (32) in Robinson and Welander (1963). There are apparently two arbitrary parameters, $r$ and $m$. However, the boundary conditions introduce a difficulty. From (C3) and (2.6) we note that the density is

$$\rho = \rho_0[1 + \epsilon(D/l)^m(y/a)^r G_{\zeta\zeta}(\zeta)] \tag{C5}$$

and, thus no matter what the asymptotic behavior of $G_{\zeta\zeta}$ as $\zeta \to \infty$, it is impossible to recover the resting stratification (2.5) at great depths. If one accepts this as an appropriate boundary condition as $\zeta \to \infty$, then (C3) cannot be used to simplify the partial differential equation (2.12). Thus, (C4) is not consistent with the boundary conditions.

To circumvent this difficulty one might attempt to generalize (2.15) by combining it with (C3)

$$M(y,\zeta) = [\zeta^{m+2}/(m+1)(m+2)] + (y/a)^r N(\zeta)$$
$$A(y) = (y/a)^{-r} \tag{C6}$$

so that once again $N$ is essentially the difference between $M$ and its asymptotic ($\zeta \to \infty$) value. Substitution of (C6) into (2.12) shows that the $y$ dependence "cancels" only if $m = 0$, i.e. only if the abyssal fluid has uniform density $\rho_0(1 + \epsilon)$. The equation for $N$ is then

$$r\zeta(N'N''' - N''^2) + rN'N'' + (2N - \zeta N')N''' = -N^{iv} \tag{C7}$$

and the boundary conditions are

$$N(0) = N_0, \quad N''(0) = -1, \quad N'(\infty) = 0. \tag{C8}$$

The first boundary condition controls the strength of the Ekman pumping. The second two concern the density field. In terms of $N$ this is

$$\rho = \rho_0[1 + \epsilon + \epsilon(y/a)^r N''(\zeta)]$$

so that from (C8b), $\rho = \rho_0$ at $y = a$, $z = 0$. Because of (C8c) $\rho = \rho_0(1 + \epsilon)$ as $\zeta \to \infty$. If $r > 0$ then (unrealistically) the surface density decreases as one moves northwards. If $r < 0$ then the density increases to the north and approaches the abyssal value, $\rho_0(1 + \epsilon)$. In this case however the distribution becomes unrealistic as one moves towards the equator and there is a singularity at the equator.

It is difficult to decide whether these difficulties are intrinsic to (2.12) or if they follow from an "unnatural" assumption about the structure of the solution [Eq. (C3) or (C6)] which artificially restricts the boundary conditions. We're inclined to speculate that this latter alternative is the case. After all, (2.12) with $M_y = 0$ does reduce to the physically sensible problems discussed in sections 2 through 4. More general and realistic surface density distributions may unavoidably require solving the partial differential equation (2.12) numerically.

## APPENDIX D

### Details of the Transition Region ($m = 0$)

This appendix discusses the mathematical details used to obtain (3.7).

To analyze the transition region at $\zeta = \zeta_*$, begin by rescaling (3.1), guided by (3.5)

$$\left.\begin{aligned} P &\equiv N/\zeta_*^2 \\ \zeta &\equiv \zeta/\zeta_* \end{aligned}\right\}. \tag{D1}$$

One finds

$$(2P - \xi P_\xi)P_{\xi\xi\xi} = -\delta P_{\xi\xi\xi\xi}$$
$$\delta \equiv (-2N_0)^{-3/2} = \zeta_*^{-3} \tag{D2}$$

as the rescaled equation.

Now it is convenient to use

$$\omega \equiv 2P - \xi P_\xi \tag{D3}$$

as a new independent variable. Essentially $\omega$ is the vertical velocity and, in terms of this variable, (D2) is reduced to a third-order equation

$$(\delta - \xi\omega)\omega_{\xi\xi} = \delta\xi\omega_{\xi\xi\xi}$$
$$\omega(0) = -1, \quad \omega'(\infty) = 0. \tag{D4}$$

It is now straightforward to recover the equivalent of (3.5a) in terms of $\omega$ and $\xi$. A regular perturbation expansion of (D4) is

$$\omega = \omega_0 + \delta\omega_1 + \cdots \tag{D5}$$

and the leading order solution is

$$\omega_0 = -1 + \xi, \quad \xi < 1. \tag{D6}$$

Further, one finds that all the higher order terms are zero. Thus the corrections to (D6), which are introduced by the internal boundary layer at $\xi = 1$, are exponentially small.

A precise analysis of the "lower outer" solution (3.5b) is straightforward and will be deferred until after the treatment of the "inner boundary layer" at $\xi = 1$.

In this region one searches for a balance in (D4) using the simplest possible rescaling

$$\left.\begin{aligned} \omega &= \delta^m\Omega(\eta) \\ \eta &= (\xi - 1)/\delta^n \end{aligned}\right\}. \tag{D7}$$

The scaling exponents, $m$ and $n$, are determined by two requirements. First, the most highly differentiated terms in (D4) balance, and this implies $m + n = 1$. Second, the outer limit of the inner solution ($\eta \to -\infty$) must match the inner limit of the outer solution ($\xi \to 1$). This implies $m = n$ so that $m = n = \frac{1}{2}$ in

(D7). The inner problem is now reduced using a regular perturbation expansion

$$\Omega = \Omega_0 + \delta^{1/2}\Omega_1 + \cdots \tag{D8}$$

and the leading order equation is

$$\Omega_0\Omega_0'' = -\Omega_0'''$$

$$\Omega_0'(\infty) \to 0 \quad \text{and} \quad \Omega_0(-\infty) \to \eta \tag{D9}$$

where the prime denotes an $\eta$-derivative. The boundary conditions in (D9b) are that "above" the internal boundary layer ($\xi \ll 1$ or $\eta \to -\infty$) one matches (D6) or equivalently (3.5). Below the internal boundary layer ($\xi \gg 1$ or $\eta \to \infty$):

$$\Omega_0 \to c \quad \text{as} \quad \eta \to \infty \tag{D10}$$

where $c$ is an unknown constant determined by numerically solving (3.15). After reversing the various scalings which led to (D9) this constant is related to the asymptotic value of the vertical velocity at $z = -\infty$. The numerical calculation of $c$ from (D9) is very easy and in fact can be done using an initial value method, i.e., (D9) can be rearranged so as to avoid the numerical solution of a two-point boundary value problem. The details have been relegated to appendix C and the result of the calculation is $c = 0.87574$.

The problem for $\Omega_1$ is now linear:

$$\Omega_1''' + \Omega_0\Omega_1'' + \Omega_1\Omega_0'' = \Omega_0''$$

$$\Omega_1(-\infty) \to 0, \quad \Omega_1'(\infty) \to 0.$$

By inspection, the solution of this equation is

$$\Omega_1 = 1 - \Omega_0'$$

so that $\Omega_1 \to 1$ as $\eta \to \infty$. This exact solution is really not as remarkable as it first seems. Specifically, note that

$$\Omega = \Omega_0 + \delta^{1/2}(1 - \Omega_0') + O(\delta)$$

$$= \Omega_0(\eta - \delta^{1/2}) + \delta^{1/2} + O(\delta)$$

and the implication of this Taylor series "reconstitution" is that the zero-order solution made an $O(\delta^{1/2})$ error in the *location* of the boundary layer. This error is corrected at next order. Aside from this we also have an improved estimate of the asymptotic value of $\Omega$ as $\eta \to \infty$, i.e.

$$\Omega \to 0.87574 + \delta^{1/2}. \tag{D11}$$

The constant $c$ in (D10), and the correction in (D11), are "inner boundary conditions" for the lower, outer problem. Because $m = \frac{1}{2}$ in (D12), and $\Omega \to c$ as $\eta \to \infty$, we see that

$$\omega \to c\delta^{1/2} \quad \text{as} \quad \xi \to 1. \tag{D13}$$

Hence, in the lower outer region, $\xi > 1$, $\omega$ must be expanded as

$$\omega = \delta^{1/2}\omega_1 + \delta\omega_2 + \cdots. \tag{D14}$$

The leading term from (D4a) is then

$$-\xi\omega_1\omega_{1\xi\xi} = 0 \tag{D15}$$

and so to satisfy the boundary condition in (D13), $\omega_1 = c$ and the deep velocity is a constant. Likewise $\omega_2 = 1$.

This completes our analysis of the almost-ideal limit. In order to compare the results of this theory with the numerical solution of (3.1) in Figs. 3 to 5 we must reverse the various scalings. It is sufficient to note that the asymptotic value of $N$ as $\zeta \to \infty$ is given by

$$N_\infty = \frac{1}{2}\delta^{-1/6}\Omega_\infty = \frac{1}{2}\zeta_*^{1/2}\Omega_\infty. \tag{D16}$$

## REFERENCES


Batchelor, G. K., 1967: *An Introduction to Fluid Dynamics.* Cambridge University Press, 615 pp.

Cox, M. D., and K. Bryan, 1984: A numerical model of the ventilated thermocline. *J. Phys. Oceanogr.*, **14,** 674–687.

Gill, A. E., 1985: An explicit solution of the linear thermocline equations. *Tellus,* **37A,** 276–285.

——, and R. K. Smith, 1970: On similarity solutions of the differential equation $\psi_{zzzz} + \psi_x = 0$. *Proc. Cambridge Philos. Soc.,* **67,** 163–171.

Huang, R. X., 1986: Solutions of the ideal fluid thermocline with continuous stratification. *J. Phys. Oceanogr.,* **16,** 39–59.

Ierley, G. R., and O. G. Ruehr, 1985: Analytic and numerical solutions of a nonlinear boundary layer problem. Submitted to *Stud. in Appl. Math.*

Killworth, P., 1983: Some thoughts on the thermocline equations. *Ocean Modelling,* **48,** 1–5.

Luyten, J. R., J. Pedlosky and H. Stommel, 1983: The ventilated thermocline. *J. Phys. Oceanogr.,* **13,** 292–309.

Needler, G. T., 1967: A model for thermohaline circulation in an ocean of finite depth. *J. Mar. Res.,* **25,** 329–342.

Pedlosky, J., and W. R. Young, 1983: Ventilation, potential—vorticity homogenization and the structure of the ocean circulation. *J. Phys. Oceanogr.,* **13,** 2020–2037.

Rhines, P. B., and W. R. Young, 1982: A theory of the wind—driven circulation I. Mid-ocean gyres. *J. Mar. Res.,* **40**(Suppl.), 559–596.

Robinson, A. R., and H. Stommel, 1959: The ocean thermocline and associated thermohaline circulation. *Tellus,* **11,** 295–308.

——, and P. Welander, 1963: Thermal circulation on a rotating sphere; with application to the oceanic thermocline. *J. Mar. Res.,* **21,** 25–38.

Stommel, H., and J. Webster, 1962: Some properties of the thermocline equations in a subtropical gyre. *J. Mar. Res.,* **20,** 42–56.

Tziperman, E., 1986: On the role of interior mixing and air–sea fluxes in determining the stratification and circulation of the oceans. *J. Phys. Oceanogr.,* **16,** 680–693.

Veronis, G., 1969: On theoretical models of the thermocline circulation. *Deep Sea Res.,* **16**(Suppl.), 301–323.

Welander, P., 1971a: The thermocline problem. *Phil. Trans. Roy. Soc. London* **A270,** 415–421.

——, 1971b: Some exact solutions to the equations describing an ideal fluid thermocline. *J. Mar. Res.,* **21,** 25–38.